Surface Modification of Polyvinyl Chloride Sheets via Growth of Hydrophilic Polymer Brushes

Yuquan Zou,[†] Jayachandran N. Kizhakkedathu,*[,†] and Donald E. Brooks*[,†,‡]

Centre for Blood Research and Department of Pathology and Laboratory of Medicine and Department of Chemistry, University of British Columbia, 2350 Health Sciences Mall, Vancouver, B.C., V6T 1Z3, Canada

Received November 14, 2008; Revised Manuscript Received January 9, 2009

ABSTRACT: Poly(*N*,*N*-dimethylacrylamide) (PDMA) brushes were successfully grown from polyvinyl chloride (uPVC) sheets via well-controlled surface-initiated atom transfer radical polymerization (SI−ATRP). An ATRP initiator containing a chloropropionate moiety was chemically tethered onto the surface of PVC via a novel wet chemical modification. Negatively charged sulfate groups were introduced to facilitate polymerization. By incorporating a chemically cleavable group into the initiator, molecular weight, polydispersity and graft density of a series of PDMA brushes synthesized on the flat surface were unambiguously characterized for the first time by gel permeation chromatography. ATR−FTIR, contact angle, SEM and AFM were used to characterize the PDMA grafted surfaces. Reaction conditions such as monomer concentration, reaction time, copper(II) concentration and salt additives were varied to systematically investigate their effects on molecular weight and graft density of the PDMA grafted from PVC. Molecular weights of grafted PDMA brushes varied from ca. 20 000 to 2 170 000 Da, while graft density ranged from 0.08 to 1.13 chains/nm^2. Polydispersity of grafted PDMA brushes was controlled between 1.20 and 1.60 by Cu(II) complex addition. Kinetic studies revealed that the surface initiation was a slow process and graft density increased during the reaction. The brush uniformity increased with increasing reaction time. Reinitiation of the obtained PDMA brushes was demonstrated, suggesting that the polymerization is "living". The successful growth of a PDMA-*b*-poly(*N*-isopropylacrylamide) (PNIPAM) copolymer brush was verified by GPC and AFM.

1. Introduction

For several decades, a great deal of research has focused on the modification of polymeric material surfaces[1,2] in attempts to control their interfacial properties since these dominate their performances when contacting biofluids, in particular, blood. For example, surface coatings of biomacromolecules such as albumin[3,4] and heparin[5−7] have been widely studied. It is generally accepted that these chemically tethered or physically adsorbed biomacromolecules can function as protecting layers to prevent undesirable events when polymers come into contact with biological fluids. A major stipulation for the use of these biomacromolecules is that their original conformation and activity after modification must be maintained. Moreover, tethered biomacromolecules must be inert to enzymatic degradation in biofluids.[8] These somewhat stringent requirements make this approach very challenging. In contrast, a more convenient approach involves coating with synthetic polymers.[9] Two of the better studied synthetic polymers are poly(ethylene glycol) (PEG) and phospholipid-like polymers, such as poly(methacryloyl phosphoryl-choline) (PC polymers). In the case of PEG, high kinetic chain mobility and a strong thermodynamic exclusion tendency makes PEG coatings of sufficient density resistant to protein adsorption.[10−13] PC polymers also show good biocompatibility since they interact only mildly with proteins and cells.[14−16]

Another promising approach emerged recently to improve the antifouling ability of polymeric materials by grafting a dense polymer layer—a polymer brush—to the surface through either covalent bonding or physical adsorption. The chemical nature of the brush and the graft density are important factors for controlling the resulting interfacial properties.[17−20] To achieve densely grafted brushes, the "grafting from" is a more widely used approach than "grafting to" due to its better control over graft density and thickness. Therefore, there has been increased attention paid to surface-initiated polymerization (SIP).[21] In this technique, initiator groups are bound to the substrate prior to the growth of polymer chains. Different polymerization techniques including radical, cationic, anionic, ring-opening metathesis (ROMP), reversible addition−fragmentation chain transfer (RAFT), nitroxide-mediated radical polymerization (NMRP), and atom transfer radical polymerization (ATRP) have been employed to achieve controlled surface polymerization.[22−28]

Of these methodologies, ATRP has proven to be very efficient and versatile[29] and carries the advantage that it can be carried out in aqueous solutions under mild conditions, which is useful when preparing hydrophilic polymers. To date, many different ATRP active monomers or macromers have been used for the surface modification of polymeric materials including poly(ethylene glycol) methacrylate (PEGMA), [30] linear and hyperbranched glycopolymers,[31,32] *N*-ispropylacrylamide (NIPAM), [33−35] 2-methacryloloxyethyl phosphorylcholine,[36] styrene,[37] 2-hydroxyethyl methacrylate (HEMA),[38,39] acrylamide,[40] and *N*,*N*-dimethylacrylamide (DMA).[41,42] Although there are many reports employing surface-initiated ATRP (SI−ATRP) to graft polymer brushes from flat surfaces such as silicon[33,37,43−46] and glass slides,[38] systematic studies of the properties of such surface grafted polymer chains are rarely reported due to complications associated with the limited amount of polymer available for analysis.

To circumvent this problem the current practice is generally to equate the properties of the solution polymers that generally form in coincidence with surface initiated polymer for ease of analysis.[46,47] Such analyses often fail to take into consideration of the properties of surfaces to which the initiators are attached, however, some of which can have a profound effect on surface

* Address to which correspondence should be addressed: E-mail: (D.E.B.) don.brooks@ubc.ca or (J.N.K.) jay@pathology.ubc.ca. Telephone: +1-604-822-7081. Fax: +1-604-822-7635.

[†] Centre for Blood Research and Department of Pathology and Laboratory of Medicine, University of British Columbia.

[‡] Department of Chemistry, University of British Columbia.

10.1021/ma8025699 CCC: $40.75 © 2009 American Chemical Society
Published on Web 04/09/2009

Scheme 1. Synthesis of 1-Sulfate-2,3-epoxypropane

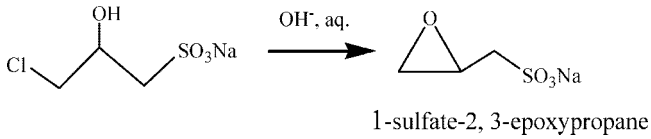

1-sulfate-2, 3-epoxypropane

initiation and polymer growth. Such effects are more evident and important in aqueous media where the nature of the charges, hydrophobicity or hydrophilicity of the surface can play a major role in the interaction of a polymerization catalyst or a hydrophilic monomer with the surface, unlike in organic media. These complex effects have not yet been incorporated into models of SIP reactions and the mechanism of surface initiated polymerization remains unclear, especially under aqueous conditions. Experimental examination of all the parameters involved in the polymerization is therefore required. This is possible only if the absolute characterization of surface attached polymer chains is carried out.

PVC is one of the most widely used thermoplastics in the world and PVC tubes and bags are the most common materials used for blood transfusion, storage and hemodialysis. When contacted with blood, PVC tends to activate a series of adverse reactions including complement activation,[48] platelet activation, adhesion and aggregation, and thrombus formation[49,50] due to its thrombogenic nature. We feel that by introducing nonionic hydrophilic brushes into the PVC−blood interface hemocompatibility of the PVC surface can be significantly improved.

Previous research from our group demonstrated the successful surface-initiated ATRP of *N*,*N*-dimethylacrylamide (DMA) and NIPAM on negatively charged polystyrene latex particles.[35,41,42] The approach showed good control over molecular weights and polydispersity for PDMA and PNIPAM brushes. In this paper, we report for the first time the controlled ATRP of DMA from a poly(vinyl chloride) (PVC) surface. Our main objective is to develop a reliable, controlled method to grow PDMA brushes from PVC via SI−ATRP. Toward this end, we have developed a novel surface modification strategy for introducing initiators to a PVC surface. A thorough understanding of the surface initiation and polymer growth is obtained by measuring the molecular weights, polydispersity, and graft density of the polymer chains grown from the PVC sheets.

2. Experimental Section

2.1. Materials and Methods. Unplasticized PVC (uPVC) sheets were purchased from Goodfellow Cambridge Limited (U.K.) with 200 μm thickness. *N*,*N*-Dimethylacrylamide (DMA) (Aldrich, 99%) was purified by vacuum distillation and stored under argon at −20 °C until use. 2-Chloropropionyl chloride (Aldrich, 97%), 1,1,4,7,10,10-hexamethyltriethylenetetramine (HMTETA, Aldrich, 97%), CuCl (Aldrich, 99+%), $CuCl_2$ (Aldrich, 99.99%) and Cu (Aldrich, 99.7%) were used as supplied. All other commercial reagents were purchased from Aldrich of the highest purity and used without further purification. Water was purified using a Milli-Q Plus water purification system (Millipore Corp., Bedford, MA) and was used in all experiments. Nuclear magnetic resonance (NMR) was performed on a Bruker AV 400 MHz NMR spectrometer at 300K. Surface functional characteristics were evaluated using attenuated total reflectance Fourier transform infrared (ATR−FTIR); the spectrum was collected on a Thermo-Nicolet Nexus FT-IR spectrometer with a MCT/A liquid nitrogen cooled detector, KBr beamsplitter and MKII Golden Gate single refection attenuated total reflectance accessory (Specac Inc.).

Synthesis of 1-Sulfate-2,3-epoxypropane (SEP). The synthesis is illustrated in Scheme 1. A 10 g sample of 3-chloro-2-hydroxypropanesulfonic acid, sodium salt hydrate, was dissolved into 40 mL of water and to this solution was added dropwise 2.6 g of sodium hydroxide, which was predissolved into 20 mL of water. The reaction proceeded at room temperature for 30 min. Almost quantitative conversion was obtained. The resulting solution was neutralized and used directly for reaction. The structure of SEP was verified by ^{1}H NMR (D_2O): $CH-CH_2-O$ δ 3.0 (m, 2H), $-O-CH-(CH_2)_2-$ δ 2.76 (t, 1H), $-CH-CH_2-SO_3Na$ δ 3.40 (t, 1H), 3.22 (t, 1H).

2.2. Surface Modification of PVC. *a. Introduction of Amino Groups—Preparation of 4-Mercaptobenzyl Amino-PVC (PVC−NH_2).* All uPVC sheets were thoroughly washed and sonicated in water prior to usage. Cleaned uPVC was cut into 5 cm × 5 cm squares and placed in a homemade Teflon mold, which ensures efficient exchange of reactant and prevents surface damage of PVC caused by a magnetic stirring bar. To a 500 mL reactor were added 80 mL of Milli-Q water and 200 mL of dimethylformamide (DMF) containing 20 g of 4-aminothiophenol and mixed well. The Teflon mold was placed into the reactor and temperature was adjusted to 50 °C. The reaction proceeded for 24 h with stirring using a magnetic bar. Modified PVC was sonicated and washed thoroughly in ethanol and finally stored in Milli-Q water until use. The modified surface was characterized by ATR−FTIR, contact angle, and XPS.

b. Incorporation of Hydroxyl (PVC−OH) and Hydroxyl plus Sulfate Groups (PVC−Sulfate−OH). The synthesis is illustrated in Scheme 2. To a 500 mL reactor was added 200 mL of DMF. Either 6 g of glycidol (80 mmol) or 6 g of glycidol mixed with 8 g of 1-sulfate-2,3-epoxypropane (SEP) (40 mmol) was diluted with Milli-Q water to 80 mL and mixed with 200 mL of DMF. PVC−NH_2 in a Teflon mold was put into a reactor and reaction allowed to proceed at 50 °C for 24 h. The reacted PVC samples were thoroughly washed with water and stored in water until use. Modified surfaces were characterized by ATR−FTIR, contact angle, and XPS.

c. Incorporation of Chloropropionate Group onto PVC Surface (PVC−CP). To a dry, 500 mL reactor were added 250 mL of hexane and 10.5 mL of triethylamine. The reactor was cooled with an ice bath, and 6.2 mL of 2-chloropropionyl chloride was added dropwise with stirring. The Teflon mold carrying PVC−OH or PVC−Sulfate−OH was placed into the reactor and the reaction allowed to proceed at 0 °C for 15 min and subsequently 12 h at ambient temperature. Modified PVC was thoroughly rinsed and extracted with ethanol and water. The modified surfaces were characterized by ATR−FTIR, contact angle, and XPS.

d. SI−ATRP. All polymerizations were carried out in a glovebox filled with argon at room temperature. Water was degassed with argon for 2 h before use. In a typical reaction, 20 mL of 1 wt % to 10 wt % DMA/H_2O solution was added into a sample vial. Then, 5 mg of Cu^ICl (2.5 μmol/mL), 10 mg of $Cu^{II}Cl$ (3.7 μmol/mL), 2 mg of Cu (1.5 μmol/mL), and 40 mg of HMTETA (8.7 μmol/mL) were added to the solution and mixed well. ATRP initiator tethered PVC samples were cut into 2 cm × 2 cm squares, placed into sample vials, and swirled gently. The reaction proceeded at ambient temperature (22 °C) for a given time, after which PVC samples were washed thoroughly with water and sonicated for 30 min prior to being stored in water. No swelling of the PVC sheet was observed during aqueous SI−ATRP.

Polymerization conditions were changed using different monomer and catalyst concentrations, and by addition of sodium chloride. The kinetics of polymerization were followed by taking out PVC samples from the polymerization vessel at different periods of time and cleaning, following a similar procedure to that above.

e. Control Experiments. Unmodified PVC was reacted with 2-chloropropionyl chloride in hexane in the presence of triethylamine for 12 h then washed thoroughly with ethanol and water. The resulting PVC sample was added to a solution containing ATRP catalyst and monomer. The concentrations of catalyst and monomer were the same as described in section d. After 24 h, the PVC sample was cleaned and vacuum-dried. As a control, unmodified PVC was subjected to similar ATRP conditions as above, except no reaction of 2-chloropropionyl chloride was carried out. The PVC sample was cleaned, vacuum-dried, and characterized by ATR−FTIR.

Scheme 2. Incorporation of Amino, Sulfate, and Hydroxyl Groups onto PVC

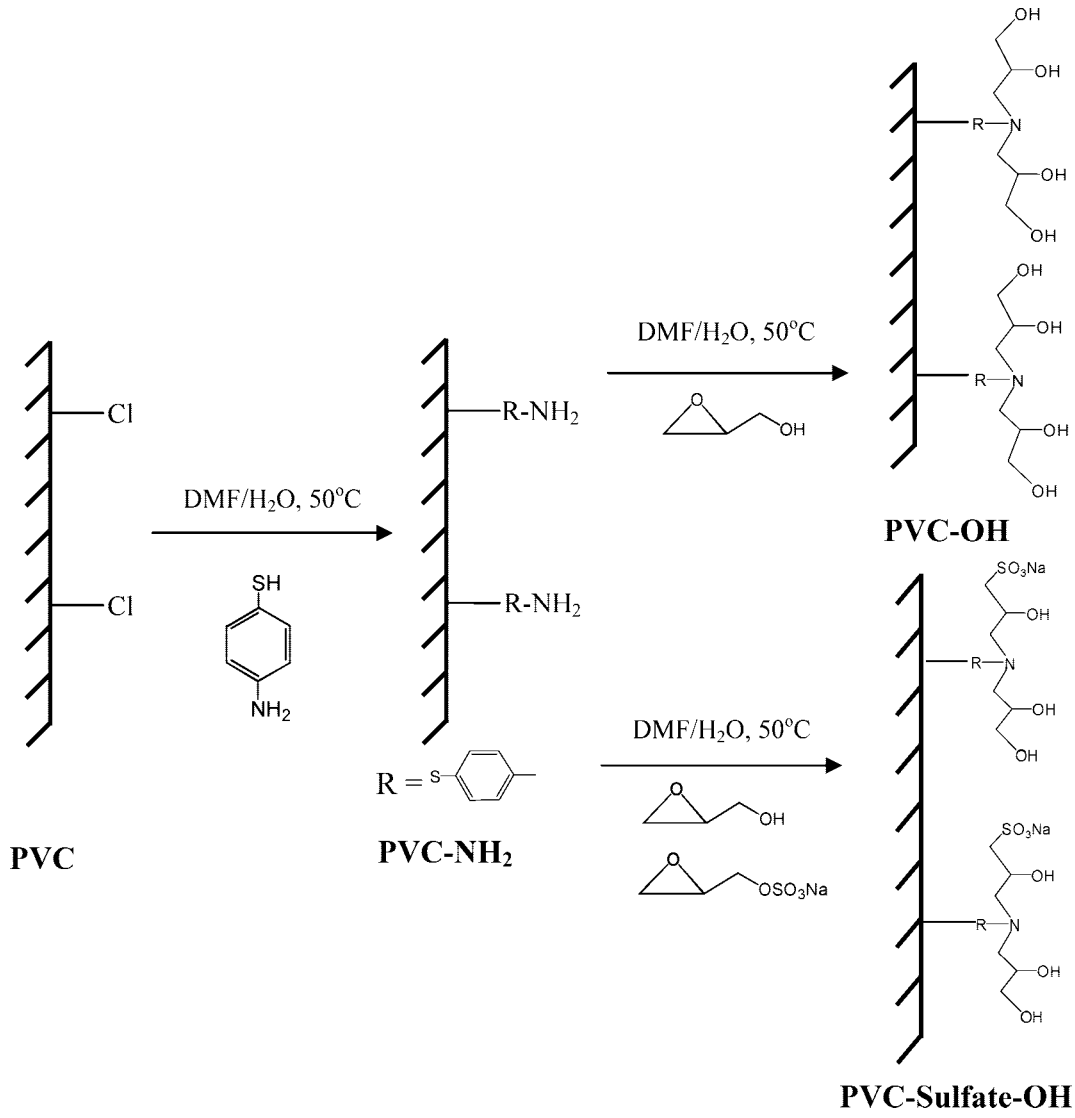

2.3. Surface Characterization of PDMA Grafted PVC. *a. Cleavage of Poly(N,N-dimethylacrylamide) (PDMA) Brush from PVC Surface.* PDMA brushes grown from a PVC surface were cleaved with a 1 M NaOH solution at ambient temperature (22 °C) under stirring. PVC samples were first cut into small pieces before hydrolysis. After 4 days of hydrolysis, the supernatant of the reaction was quantitatively taken out and dialyzed against water for 5 days. The dialyzed solution was lyophilized and reconstituted in a given amount of 0.1 M $NaNO_3$ solution. Molecular weight, polydispersity, and absolute weight of surface polymer were characterized by GPC. The graft density of PDMA was calculated using the following equation:

$$\sigma = \frac{W \times N_A}{M_n \times A} \quad (1)$$

Here σ = graft density (chains/nm^2), W = absolute weight of cleaved polymer; N_A = Avogadro's constant, M_n = number average molecular weight, and A = surface area of PVC (two sides).

The mass of cleaved PDMA brushes was determined by a calibrated refractive index (RI) detector. The TDA-300 RI used in this study can detect down to the 10^{-5} to 10^{-6} g level, which generally gave satisfactory accuracy from the RI signal for our cleaved samples.

An example of cleavage and calculation of the graft density is given below. Three pieces of PDMA brush grafted PVC sample (2 cm × 2 cm square each, total surface area (both sides) was 24 cm^2) were cut into small pieces and stirred in 5 mL of 1 M NaOH for 4 days. The supernatant was quantitatively removed, dialyzed against water for 5 days, and freeze-dried to remove water. The obtained PDMA was reconstituted into 400 μL of 0.1 M $NaNO_3$ solution. 200 μL of this solution was injected through the GPC column and the M_n (56 000 Da) and absolute amount of PDMA (6 × 10^{-5} g) was determined. From these values, the graft density for the sample was calculated as 0.54 chains/nm^2.

b. Water Contact Angle Measurements. Modified PVC and PVC−PDMA brush samples were characterized by static water contact angle measurement. A water droplet of 2 uL was placed on the surface and an image of the droplet was taken with a digital camera (Retiga 1300, Q-imaging Co.). The contact angle was analyzed using Northern Eclipse software. Five different sites were tested for each sample.

c. UV−Vis. The surface concentration of tethered mercaptobenzyl amino groups was measured by UV−vis spectroscopy. Equimolar amounts of PVC and PVC−NH_2 were dissolved into THF followed by precipitation in acetone. This process was repeated for 3 times to remove any free aminothiophenol and residual plasticizer. Purified equimolar PVC and PVC−NH_2 powder were dissolved in THF and analyzed by UV−vis spectroscopy. The amount of tethered mercaptobenzyl amino group was obtained by subtraction of the PVC absorbance from that of the PVC−NH_2. 4-Ami-

Scheme 3. Incorporation of an ATRP Initiator onto PVC and SI−ATRP from PVC

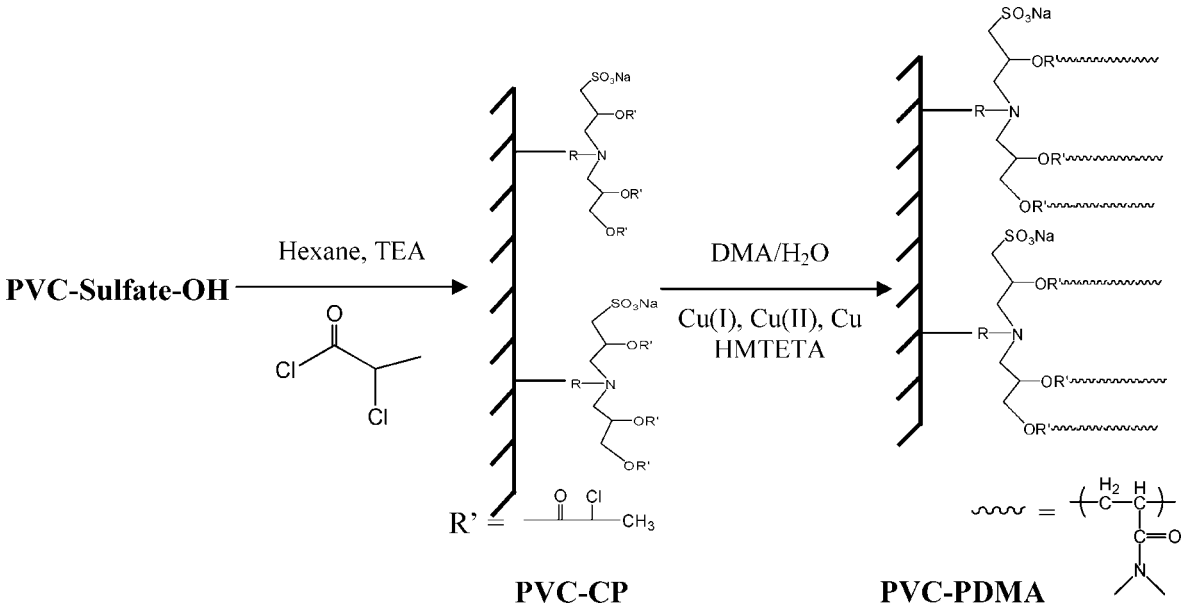

nothiophenol solutions of known concentrations were used for calibration standards at wavelength of 300 nm.

d. XPS Measurements. X-ray photoelectron spectroscopy (XPS) was performed using a Leybold LH Max 200 surface analysis system (Leybold, Cologne, Germany) equipped with a Mg Kα source at a power of 200 W. Elements were identified from survey spectra. High resolution spectra were also collected at 48 eV pass energy. Prior to XPS analysis, all samples were thoroughly dried in a vacuum.

e. AFM. Atomic force microscopy (AFM) measurements were performed on a multimode, Nanoscope IIIa controller (Digital Instruments, Santa Barbara, CA) equipped with an atomic head of 100 × 100 μm^2 scan range. AFM was performed in air or under water in contact mode using a commercially manufactured V-shaped silicon nitride (Si_3N_4) cantilever with gold on the back for laser beam reflection (Veeco, NP-S20). Typical tip radius and spring constant of the cantilever was 5−40 nm and 0.06 N/m respectively.

Force measurements were performed using AFM and a fluid cell containing 100 mM NaCl solution freshly prepared with Milli-Q water. The experiments were performed in force mode. The onset of the region of constant compliance was used to determine the zero distance, and the region in which force was unchanged was used to determine the zero force. All measurements were taken at an approach rate of 1.0 Hz. The raw AFM force data (cantilever deflection vs displacement data) were converted into the reduced force vs separation following the principle of Ducker et al.[59]

f. GPC−MALLS. Absolute molecular weights of the polymers were determined by gel permeation chromatography (GPC) on a Waters 2690 separation module fitted with a DAWN EOS multi-angle laser light scattering (MALLS) detector from Wyatt Technology Corp. with 18 detectors placed at different angles (laser wavelength $\lambda = 690$ nm) and a refractive index detector from Viscotek Corp. operated at $\lambda = 620$ nm. 0.1 M $NaNO_3$ aqueous solution was used as the mobile phase at a flow rate of 0.8 mL/min. Aliquots of 200 μL of the polymer solution were injected through Ultrahydrogel columns at 22 °C (guard column, Ultrahydrogel linear with bead size 6−13 um, elution range 10^3 to 7 × 10^6 Da and Ultrahydrogel 120 with bead size 6 um, elution range 150 to 5 × 10^3 Da connected in series; from Waters). The d*n*/d*c* value for PDMA in 0.1 M $NaNO_3$ was determined at $\lambda = 620$ nm as 0.150 mL/g (determined online using the RI detector response from a number of different concentrations of pure polymer), which was used for calculating the molecular weight parameters.[41,42]

Results and Discussion

3.1. Incorporation of ATRP Initiators onto PVC Surface via a Wet Chemical Method. One of the challenges in preparing surface grafted polymer brushes from a flat surface is to introduce densely tethered ATRP initiators. Different approaches employed to introduce densely tethered ATRP initiators include the Langmuir−Blodgett technique and chemical modification based on the different properties of the substrate.[33,36,52,56−58] Since "dry" surface modification techniques such as gas plasma (ammonia, allylamine, oxygen) have been widely used for the initial activation in the case of PVC, the term "wet" chemical modification was used to differentiate the current process and gas plasma techniques. In the current study, the design of the synthetic procedures was based on the need to anchor chemically bonded ATRP initiators to the PVC surface. Importantly, for our purposes the initiator must also be chemically cleavable. To this end we have designed the new surface modification pathway for PVC, which is illustrated in Schemes 2 and 3. Unplasticized PVC was used to eliminate the possible interference from plasticizers during the wet modification. The modification is based on surface amination followed by a ring-opening reaction of epoxide to form reactive hydroxyl groups then incorporation of ATRP initiators. In each step the modification conditions are carefully controlled to produce maximum surface modification without affecting the bulk properties and appearance of the PVC film. Initially uPVC was reacted with 4-aminothiophenol in a mixture of DMF and water. The ratio of DMF to water, temperature, reaction time and concentration of 4-aminothiophenol have previously been reported as important parameters influencing the degree of modification.[51] A higher ratio of DMF resulted in a higher degree of modification of PVC since it acts as a good solvent for PVC. Higher temperature and longer reaction time can also result in a higher degree of modification. On the other hand, elevated temperatures and higher ratios of DMF might cause severe swelling of the PVC and subsequently compromise its mechanical properties.

Thus, a ratio of DMF to water of 2.5:1 (v/v) and a reaction temperature of 50 °C were chosen in this study. Under these conditions, PVC showed very little swelling. The thickness difference before and after reaction was less than 5%. The ATR−FTIR spectrum of the obtained PVC−NH_2 and the

difference spectrum when the spectrum of unmodified PVC was subtracted verified the successful addition of amino groups (Figure 1S). The degree of modification was estimated by UV−vis spectroscopy. Before performing UV−vis measurements, PVC−NH_2 was dissolved in THF and precipitated in acetone several times to remove possible residual free 4-aminothiophenol. Bare PVC and 4-aminothiophenol (at different concentrations) dissolved in THF were used as a background and a standard (Figure 2S) respectively. Compared to free 4-aminothiophenol, the maximum absorbance of the bonded mercaptobenzyl amino group (λ = 295 nm) was 5 nm lower, possibly due to the covalent attachment (Figure 3S). The calculated degree of modification was ca. 0.98 μmol of mercaptobenzyl amino groups/cm^2. It should be noted that the substitution of amino groups not only takes place on the surface of PVC but it could penetrate several hundred nanometers below the surface due to the solvency of DMF.

In order to generate a cleavable ATRP initiator group and to increase the amount of functionality on the surface we used an epoxide ring-opening reaction of amino groups for the next step of modification. As shown in Scheme 2, the reaction of glycidol with primary amine groups should generate four hydroxyl groups per amine on the PVC surface, potentially yielding an unprecedented high concentration of surface tethered ATRP initiators. The subsequent esterification of the hydroxyl groups generated ester bonds, which can be easily cleaved. It is important to note that ester bonds are much easier to hydrolyze than *N*-substituted amide bonds.

The current modification can also easily be adapted to the generation of negative surface charges on PVC. It is known from our previous work that surface negative charges are essential for generation of densely grafted polymer brushes in aqueous ATRP using hydrophilic monomers.[35,41,42] Sulfate groups on the surface along with hydroxyl groups were introduced to the PVC surface using a mixture of glycidol and sulfated glycidol (Scheme 2). The amount of charge on surface is controlled by changing the ratio of glycidol to 1-sulfate-2,3-epoxypropane used for the reaction. The successful addition of hydroxyl and sulfate groups was verified by XPS (Figure 4S). The effect of the sulfate groups on surface polymerization will be discussed in a later section.

To introduce the 2-chloropropionate group, hydroxyl functionalized PVC surfaces were reacted with 2-chloropropionyl chloride in hexane in the presence of triethylamine. Since hexane is a nonsolvent for PVC, we expect that this step will only modify the surface hydroxyl groups. Successful tethering of 2-chloropropionate was supported by the water contact angle measurements (Table 1S, Supporting Information). PVC and PVC−NH_2 gave contact angles of 94.5 ± 2.3 and 88.6 ± 1.2° but due to the presence of hydroxyl and sulfate groups, the water contact angle of PVC−OH and PVC−sulfate−OH were decreased to 72.6 ± 2.2 and 71.3 ± 1.4°, respectively. The contact angle of PVC−CP was then increased to 92.7 ± 1.1°, indicating the attachment of hydrophobic 2-chloropropionate groups.

More evidence for the successful tethering of surface initiators was also observed by XPS. Since the chlorine atom at the initiator group was minor and overlapped with chlorine from PVC, we conducted a control reaction to introduce 2-bromopropionate group onto the PVC surface. Figure 1 shows the XPS spectrum of PVC−ATRP containing 2-bromopropionate group. A single bromine peak (Br 3d) was observed at 71 eV, verifying a successful incorporation of ATRP initiator.

3.2. Aqueous SI−ATRP of DMA from PVC surfaces. *3.2.1. Polymerization and Cleavage of PDMA Brushes from PVC Surfaces Characterized by ATR−FTIR and NMR.* SI−ATRP of DMA from the 2-chloropropionate groups tethered onto the uPVC surface was carried out in aqueous media using

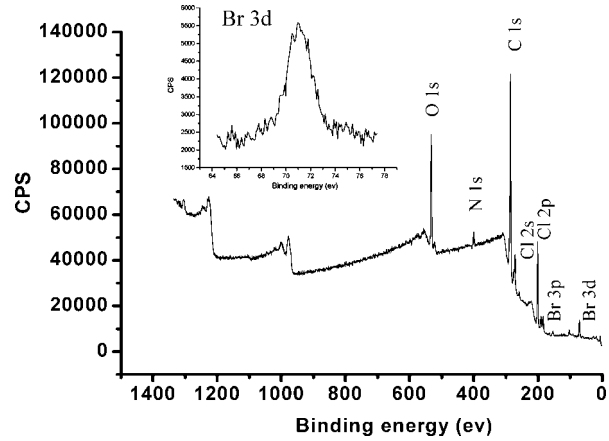

Figure 1. XPS spectrum of PVC−ATRP containing 2-bromopropionate initiators.

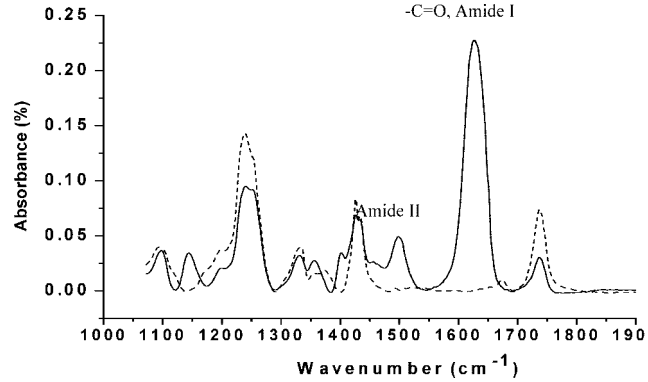

Figure 2. ATR−FTIR spectrum of PVC−PDMA before (solid line) and after hydrolysis (dashed line). The PVC−PDMA was prepared by ATRP in 3% of DMA for 72 h. Cu(I) was 2.5 μmol/mL; Cu(II), 3.7 μmol/mL; Cu, 1.5 μmol/mL, HMTETA, 8.7 μmol/mL.

Cu/HMTETA as the catalyst. Figure 2 (solid line) shows ATR−FTIR spectrum of PDMA brushes on PVC prepared from 3% DMA (wt %) at 72 h. A strong amide I absorption band was observed at c.a 1630 cm^{-1} indicating successful growth of PDMA brushes. The cleavability of the PDMA brushes was verified by basic hydrolysis and as seen from the spectrum (Figure 2, dashed line) the amide I absorption at 1630 cm^{-1} completely disappeared after cleavage, indicating complete hydrolysis of the PDMA chains from the PVC surface. Furthermore, the structure of the cleaved PDMA brush was verified by ^{1}H NMR (Figure 3). It is evident that the chemical structure of the grafted PDMA remained intact after hydrolysis compared to solution polymer, ensuring that cleaved polymer can be used to estimate properties of surface polymer. Due to the mild conditions employed for hydrolysis, no chain scission was expected. The high molecular weight of the PDMA prevented unambiguous end group analysis by NMR due to the poor resolution of the peaks. Very small peaks seen around 1.0−1.2, 1.5−2.5, and 3.2−4.0 ppm might be from the additives leached out during the cleavage of PDMA from PVC. This is supported by the fact that peaks are much narrower and sharper compared to PDMA peaks, suggesting the presence of a smaller molecular weight compound as impurity. We believe this is the first verification of the structure of cleaved polymer chains from a flat surface. We used similar conditions for further cleavage analysis of brush samples.

3.2.2. Effect of Surface Charge. We demonstrated previously that the presence of a sulfate groups can significantly improve the surface initiated polymerization from latex particles.[41,42] In the current study, we observed a similar trend as seen from the

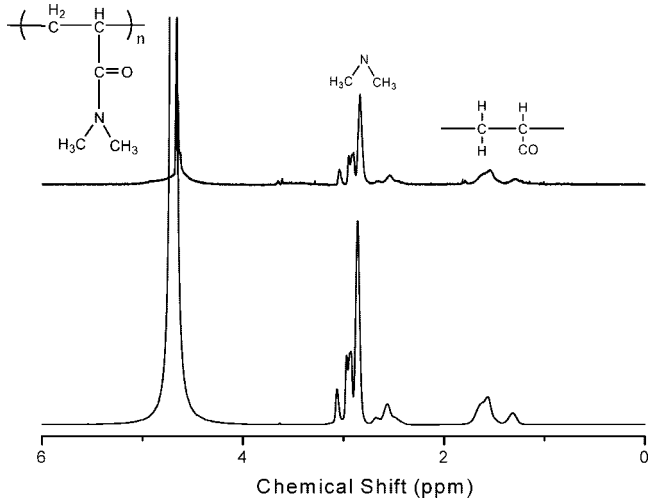

Figure 3. ^{1}H NMR of a cleaved (top, M_n = 77 000, PD = 1.83) and solution PDMA (bottom, M_n = 56, 000, PD = 1.89).

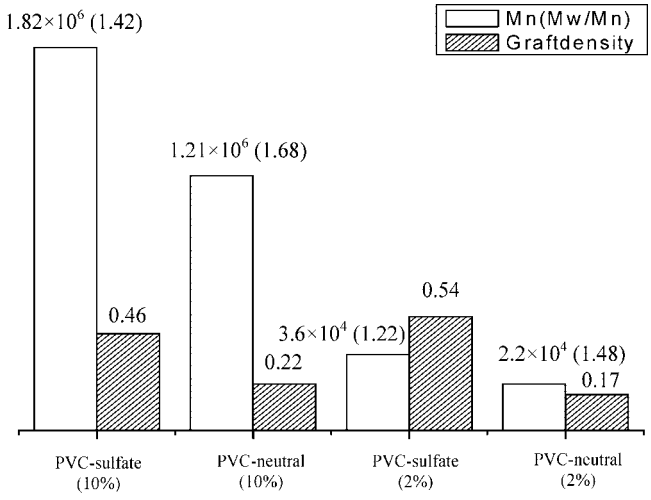

Figure 4. Comparison of molecular weight (Da) and graft density (chains/nm^2) of modified PVC with and without sulfate present on the surface. Polymerization was carried out at room temperature for 24 h (10% of DMA) and 120 (2% DMA) h, respectively. Cu(I) was 2.5 μmol/mL; Cu(II), 3.7 μmol/mL; Cu, 1.5 μmol/mL, HMTETA, 8.7 μmol/mL.

comparison of polymerization data with and without sulfate groups presented in Figure 4. This further supports the electrostatic model for the enrichment of ATRP catalyst near the surface, facilitating the initiation and polymerization.[35,41,42] when the surface was charged, the complex of Cu(I)/ligand and Cu(II)/ligand should be enriched on the surface via electrostatic interaction, which could facilitate the initiation and growth of the polymer chains. We see that sulfate incorporated surfaces gave ~2−3 times higher graft densities than surfaces without sulfate. For example at 2 wt % DMA concentration, the graft density was 0.54 chains/nm^2 for the negative surface compared to 0.17 chains/nm^2 on the neutral surface after 24 h of polymerization. Similar observations are made for 10 wt % monomer concentration. The molecular weights of PDMA from sulfate-containing surfaces were also higher than for nonsulfated surfaces, but the difference was not as significant as for graft density. Although neutral surface gave lower number average molecular weights than charged ones, the polydispersities of the PDMA chains obtained were much higher than those obtained from sulfated surface. Therefore, it was difficult to examine the real effect of surface charges on molecular weight in this study. Unless otherwise specified, the remaining polymerizations in this study were carried out on sulfate-incorporated PVC sheets.

3.2.3. Effect of the Reaction Conditions on SI−ATRP. The effects of different reaction conditions on the surface initiated polymerization are summarized in Table 1. Monomer concentration and reaction time were two important parameters affecting molecular weight and graft density of PDMA brushes. Other parameters examined include the concentration of copper(II) complex and effect of sodium chloride.

Effect of Monomer Concentration. The results given in Table 1 show that DMA concentration was a crucial parameter for controlling the molecular weight of PDMA brushes: the higher the DMA concentration, the higher the molecular weight. At 24 h for a given copper catalyst concentration, 3, 5, and 10 wt % DMA yielded surface grafted chains having molecular weights 2.8×10^4, 5.43×10^5, and 1.82×10^6 Da, respectively. This is in agreement with the theoretical expectation that at constant initiator concentration higher monomer concentration yields longer polymer chains. The effect of DMA concentration on graft density was not so straightforward. The graft densities of PDMA brushes prepared by 24 h polymerization in 3 and 5 wt % DMA in the presence of 3.7 μmol/mL of copper(II) complexes was 0.29 and 0.25 chains/nm^2 respectively. The similar values suggest that at medium to low concentration of DMA, there is little effect on graft density. However, polymerizations with a higher DMA concentration (10 wt %) produced a much denser PDMA brush (0.46 chains/nm^2) after 24 h. Possible reasons for this difference could be due to the steric effect of initiated chains on diffusion of reaction components. Matyjaszewski et al.[61] discussed similar effects on initiation efficiency caused by initiated side chains of a macroinitiator backbone and their effects on diffusion of monomer to the initiation sites. A similar argument might explain why higher monomer concentration yielded a higher graft density at a given point in the polymerization. When chain length and graft density reach a certain level, monomer diffusion through the polymer brushes is expected to be reduced. A high monomer concentration helps overcome this phenomenon. At low or medium monomer concentration, slowly initiated sites may not be able to propagate efficiently, resulting in either a low graft density or a high polydispersity after a given polymerization time.

Effect of Reaction Time. Figures 5 and 6 show the effect of reaction time on the growth of PDMA chains from the PVC surface in 10wt % DMA. The molecular weight increased sharply in the first 2 h (Figure 5), became moderate within the initial 24 h, and reached a plateau of around 2×10^6 Da after 48 h. A similar trend was observed for polymerizations carried out at lower DMA concentrations. Due to the presence of free polymer in solution, the relationship between conversion and molecular weight was not studied. The polydispersity of the chains remains almost constant (between 1.4 and 1.66) except for sample at 4 h (1.97). The results also show that under the conditions studied, the propagation rate is initially very high. For example, even at 2 h the molecular weight exceeds 5×10^5 at high monomer concentration.

Surprising results were obtained for the graft density of chains. Along with increase in molecular weight, the chain density also increased (Figure 6); from 0.08 chains/nm^2 to 1.13 chains/nm^2 at 96 h indicating slow initiation. Thus it is not surprising to see the higher polydispersity of the cleaved chains from the surface at early times; as the reaction progresses, new chains are being added to already existing chains.

Figure 7 shows the ATR−FTIR spectra of PDMA brushes synthesized at different time intervals. The intensity of the amide absorption increased with reaction time indicating that the amount of polymer on the surface increased, supporting the

Table 1. Effect of Different Reaction Conditions on Molecular Weight, Polydipersity and Graft Density of PDMA Brushes[a]

DMA(w/w %)	Cu(II)[a] (μmol/mL)	NaCl (mol/L)	time (h)	M_n ($\times 10^5$ g/mol)	M_w/M_n	graft density (chains/nm^2)
10	3.7		2	5.9	1.56	0.08
	3.7		4	4.3	1.97	0.13
	3.7		8	10.0	1.50	0.26
	3.7		24	18.2	1.42	0.46
	3.7		48	21.7	1.66	0.92
	3.7		96	20.3	1.58	1.13
	3.7	0.1	24	12.5	1.36	0.23
5	0		24	11.2	1.96	0.28
	0.74		24	7.94	1.62	0.23
	3.7		24	5.43	1.40	0.25
	3.7	0.1	24	1.98	1.88	0.12
3	0		24	0.78	1.83	0.26
	0.74		24	0.56	1.78	0.31
	3.7		24	0.28	1.54	0.29
	3.7		48	0.42	1.72	0.42
	3.7		120	0.49	1.47	0.63
	3.7		240	0.38	1.43	0.70
2	3.7	0.01	72	0.59	1.62	0.35
	3.7	0.05	72	0.62	1.70	0.23
	3.7	0.1	72	0.77	1.83	0.25
	3.7		120	0.56	1.24	0.54
	3.7		240	0.44	1.28	0.52
1	3.7		120	0.38	1.98	0.26
	3.7		240	0.52	2.22	0.42

[a] Cu^{I}Cl was 2.5 μmol/mL; Cu, 1.5 μmol/mL; HMTETA, 8.7 μmol/mL).

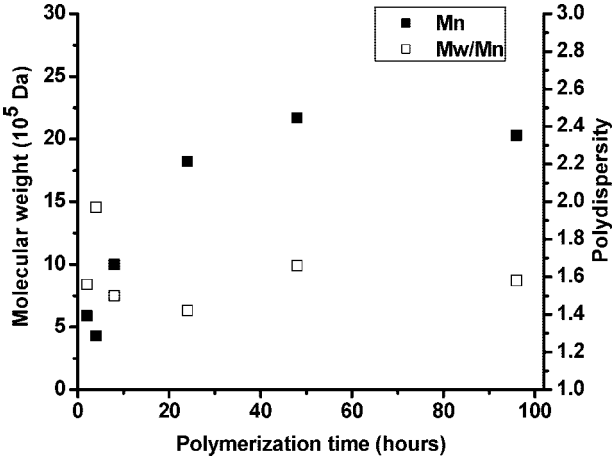

Figure 5. Dependence of molecular weight and polydispersity on polymerization time. DMA: 10% (wt %), Cu(I) was 2.5 μmol/mL; Cu(II), 3.7 μmol/mL; Cu, 1.5 μmol/mL; HMTETA, 8.7 μmol/mL.

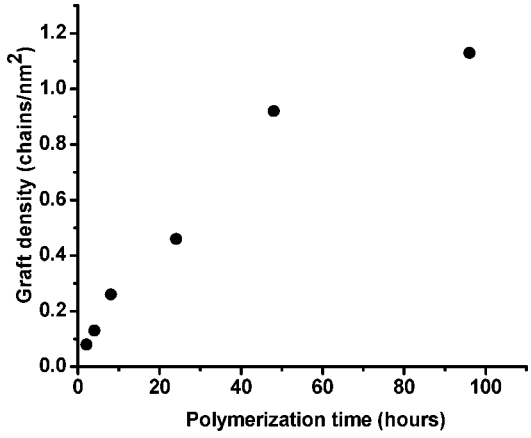

Figure 6. Dependence of graft density on polymerization time. DMA: 10% (wt %), Cu(I) was 2.5 μmol/mL; Cu(II), 3.7 μmol/mL; Cu, 1.5 μmol/mL; HMTETA, 8.7 μmol/mL.

increase of molecular weight and graft density with reaction time independently obtained from the GPC−MALLS analysis.

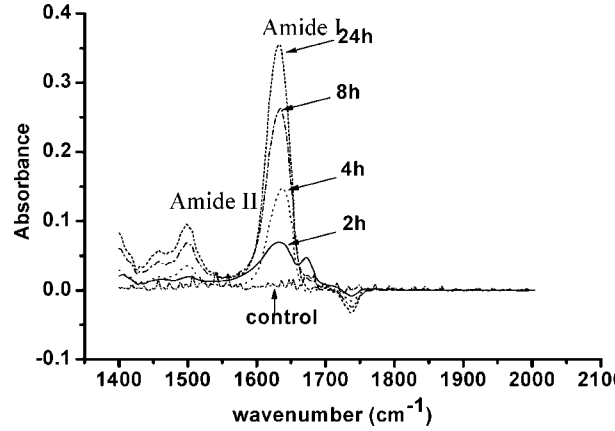

Figure 7. ATR−FTIR spectrum of PVC−PDMA brushes obtained in 10% DMA after 2, 4, 8, and 24 h. Cu(I) was 2.5 μmol/mL; Cu(II), 3.7 μmol/mL; Cu, 1.5 μmol/mL; HMTETA, 8.7 μmol/mL.

The slow initiation could be due to several factors including nonuniform surface geometry, chemical composition and local concentration of reagents at the interface. AFM morphology of the PVC modified with ATRP initiators (Figure 5S) shows the existence of microroughness on the surface, producing a potential nonuniformity of access of reagents to different parts of the surface. The surface roughness of the initiator modified PVC was increased to 42 nm compared to 8.5 nm for original PVC. This nonuniformity might be responsible for the discrepancy in initiation rates at different sites. Moreover, initiators neighboring the sulfate groups would likely have a different chemical environment (higher catalyst concentration) that could cause a different initiation rate. Another factor which might influence this is the monomer availability for the propagation of initiated radicals. The above two effects, geometry and the local chemical composition, might be exaggerated when initiated sites propagate to a degree that causes a steric effect preventing initiation or propagation of neighboring sites. A third factor which may be contributing to the slow initiation is the accessibility of highly hydrophilic reagents due to the hydrophobic initiator modified surface.

At the initial stage of polymerization, polydispersity was generally high and decreased at long times, once the graft density

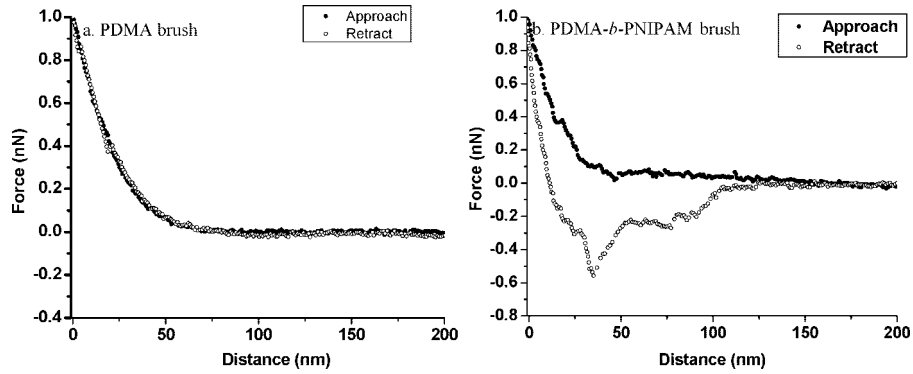

Figure 8. Force measurements for (a) PDMA and (b) PDMA-*b*-PNIPAM grafted PVC surfaces by AFM. PDMA-grafted PVC was prepared by ATRP in 3% of DMA for 240 h. PNIPAM-*b*-PDMA grafted PVC was prepared by ATRP of the PDMA grafted PVC surface described in (a) in 1 wt % PNIPAM for 12 h. Cu(I) was 2.5 μmol/mL; Cu(II), 3.7 μmol/mL; Cu, 1.5 μmol/mL; HMTETA, 8.7 μmol/mL.

and molecular weights had reached plateau values. This reflects the slow initiation rate. At early times, large amounts of newly initiated chains coexisted with propagated chains, causing a broad distribution of molecular weight. Once the graft density reaches its maximum, few if any newly initiated chains are added to the distribution and a quite uniform distribution is obtained. At low concentrations the time required for this can be very long, >240 h for the 1 wt % solution illustrated in Table 1. These results demonstrate that the surface polymerization reaction ceases at a well-defined molecular weight for a given set of conditions, producing low polydispersities (e.g., 1.2−1.3).

We believe that 1.13 chains/nm^2 is the highest graft density ever reported. Strictly speaking, this number is an overestimate in that it is based on the apparent surface area derived from the macroscopic size of the PVC samples. Due to surface roughness the true surface area, determined on a nm length scale, would be considerably larger. However, because of the high molecular weights the length scale associated with the polymer chains would be of the order of R_g, or the brush thickness, which would be on the order of 10^2-10^3 nm for the highest molecular weight and most dense brushes, which is larger than the scale of the surface rougness so the area estimate on which the surface density is calculated remains relevant. We feel the high graft densities are likely due to the high concentration of ATRP initiators on the surface produced by the synthetic design discussed in the previous section combined with the high surface concentration of catalyst caused by the presence of negatively charged sulfate groups which results in high initiation efficiency.

Our results also show that at a given monomer concentration, chain propagation became very slow after the polymerization reached a certain stage. For example, at 3 wt % DMA, the molecular weight of the brush was 79,000 Da after 120 h of ATRP, and only 85 000 Da after 240 h (Table 1). Similarly, at 10 wt % DMA, the molecular weight (M_n) was 2.17×10^6 Da after 48 h of ATRP, and only 2.03×10^6 Da after 96 h; the lower molecular weight is due to the increase of polydispersity. ^{1}H NMR of the supernatant showed that at the end of all reactions, there was still a large amount of monomer present in the system, due to the small absolute number of initiating groups in the system. Therefore, the mechanism resulting in this phenomenon is not clear. Matyjaszewski et al.[53] reported the possible loss of bromine end groups during the ATRP of DMA through a cyclization reaction in organic system, but this was not the cause in our case. To verify that the polymer chains were still "living" at the point the molecular weight plateaued, further reinitiation of the PDMA brushes was conducted, which will be discussed in the following section.

Copper (II) Complex and Salt Effect. The copper(II) complex concentration was critical for obtaining PDMA brushes with low molecular weight distribution. Table 1 shows that PDMA obtained by polymerization in 5 wt % DMA after 24 h had a polydispersity of 1.96, 1.62, or 1.40 when the copper(II) complex concentration was 0, 0.74, or 3.7 μmol/mL respectively. Similar results were observed when polymerization proceeded in 3 wt % DMA. Thus, as more copper(II) catalyst is made available, a more uniform brush layer is obtained. This finding is in agreement with the copper(II) complex functioning as a deactivator in classical ATRP. In general, by using 3.7 μmol/mL of copper(II) complex, the polydispersity of PDMA brushes could be controlled at 1.6 to 1.2, which is fairly low considering the nature of surface polymerization. It is noteworthy that in some cases, the polydispersity was quite high, however, even when using excessive amounts of the Cu(II) complex.

It was also observed that the addition of sodium chloride inhibited surface polymerization. In the presence of 0.1 M NaCl, the graft density was decreased ~50% in 10% and 5% DMA solutions; similar results were obtained for 3 wt % DMA. Molecular weight characterization also showed that PDMA obtained in the presence of NaCl gave somewhat shorter chain lengths. These observations are consistent with our earlier observations on PDMA brush synthesis by SI−ATRP from negatively charged polystyrene latex surfaces.[35,41,42] The inhibitory effect of NaCl is likely due to the screening of surface charges and reduction of surface potential by the increase in ionic strength. Reducing the magnitude of the negative surface potential is expected to decrease the surface concentration of any positively charged species in solution, in particular the Cu(I)- and Cu(II)-containing catalyst complexes. This in turn would lead to the direct effects on initiation observed. The effect on molecular weight is likely due to the reduction in propagation rate due to the increased concentration of deactivator Cu(II) complex in the presence of sodium chloride due to the common ion effect[62,63]

3.2.4. Block Polymerization of PNIPAM. To verify the "living" nature of this polymerization, a PDMA brush (M_n = 38 000 Da, M_w/M_n = 1.43, graft density = 0.70 chains/nm^2) that was stirred in water for 7 days, was used as a macroinitiator for the polymerization of *N*-isopropylacrylamide (NIPAM). This monomer was chosen due to the amphiphilicity of PNIPAM and its resulting affinity for silicon nitride AFM tips; this provides a facile method for detecting the presence of PNIPAM on a surface based on force measurements utilizing AFM in an aqueous environment.[60] Figure 8 shows force−distance measurements for PDMA (Figure 8a) and PDMA-*b*-PNIPAM (Figure 8b) grafted PVC. Due to its hydrophilic nature, PDMA brushes showed identical exponentially decaying repulsive forces during approach and retraction with the Si_3N_4 tip in water. This repulsive force is caused by steric interaction of the hydrophilic brush with the Si_3N_4 tip with no significant adsorption. This observation is in agreement with previous reports.[47,54,55] In

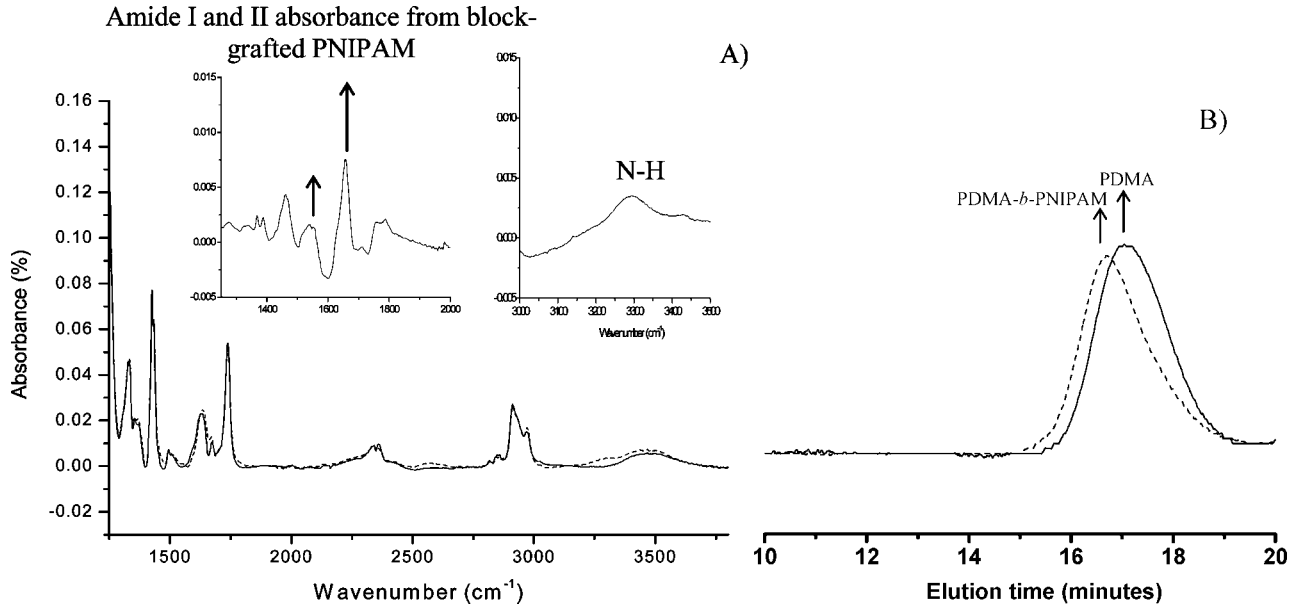

Figure 9. (A) ATR−FTIR spectrum of PDMA (solid line) and PDMA-*b*-PNIPAM grafted PVC (dotted) and subtraction of PDMA-*b*-PNIPAM by PDMA (inset). (B) GPC profiles of PDMA (solid line, M_n = 38 000 Da, M_w/M_n = 1.43, graft density = 0.70 chains/nm^2) and PDMA-*b*-PNIPAM (dotted line, M_n = 41 600 Da, M_w/M_n = 1.51, graft density = 0.68 chains/nm^2).

contrast, the PDMA-*b*-PNIPAM brushes showed a similar repulsive force during approach, but a strong adhesive force during retraction. The adhesive force was caused by the hydrophobic interaction of the PNIPAM segments and polymer adsorption on the Si_3N_4 tip.[60]

The presence of PNIPAM was also verified by ATR−FTIR. Figure 9A shows the ATR−FTIR spectrum of PDMA and PDMA-*b*-PNIPAM grafted PVC, and their difference spectrum. Absorbance bands at 3300, 1654, and 1540 cm^{-1} in the difference spectrum were attributed to the grafted PNIPAM segment. More evidence from GPC is shown in Figure 9B. Shift of the peak of RI signal from 17.1 to 16.6 min after block polymerization (M_n increased from 38 000 to 41 600 Da) and similar polydispersity (1.43 and 1.51) of the two peaks indicates the predominance of growth of PNIPAM from the PDMA chains. All these results show that the great majority of the PDMA chains remain "living" after polymerization and can be reinitiated.

3.2.5. Understanding the Growth of PDMA Brushes via GPC−MALLS. Successful recovery of surface-grafted PDMA brushes allows a thorough study of the process of polymer growth from the surface. Figure 10 presents selected GPC−MALLS profiles of cleaved PDMA brushes with medium and high molecular weights. In general, PDMA brushes obtained in relatively high DMA (4% to 10%) concentration had similar refractive index (RI) and MALLS profiles. A monomodal peak with a narrow molecular weight distribution is obtained, indicative of controlled polymerization from the surface. In each case, no low molecular weight tail was observed. However, at low DMA concentration (≤3%), the resulting PDMA gave a GPC trace with two distinct peaks.

Figure 11a shows GPC−MALLS and RI profiles for PDMA brushes prepared in 2 wt % DMA for 72 h. The GPC−MALLS profile contains two major peaks eluted at 14.8 and 16.3 min. However, a careful comparison of RI and MALLS signals reveals that only the peak at 16.3 min had a significant RI signal. It is known that RI measures the mass of eluent, while MALLS is more sensitive to its actual size (molecular weight). This finding indicates that the shoulder peak at 14.8 min is a very minor mass component. To further elucidate the ratio of these two, the same sample was analyzed with a GPC system equipped

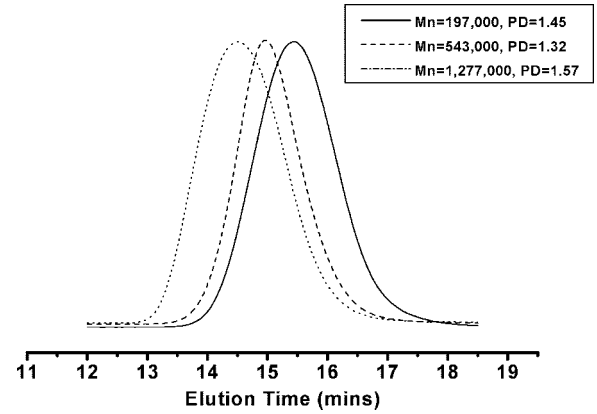

Figure 10. Selected GPC−MALLS profiles for PDMA chains having medium (∼10^5 Dalton) to high molecular weight (∼10^6 Da) grafted onto PVC surfaces.

with four columns, which gave better resolution than the two column setup we use routinely. Figure 11b shows MALLS and RI profiles of the same sample run through four columns (Ultrahydrogel linear, 2000, 1000, 500 Å pore size). MALLS shows three well resolved peaks eluted at 30, 45, and 55 min while RI only shows one major peak at 55 min. In MALLS, the shoulder peak at 14.8 min in Figure 11a was resolved to two minor peaks at 30 and 45 min while a major peak also appeared at 55 min. Due to the limited signal/noise ratio of the RI detector, it was not possible to characterize peaks 2 and 3 unambiguously. However, they should have higher molecular weights than the major peak due to their shorter elution time. The polydispersity of the major peak decreased to 1.22 after resolution. The presence of minor peaks 2 and 3 represents nonuniformity of the PDMA brushes prepared in low monomer concentration.

A longer reaction time helps to produce a more uniform brush layer. Figures 12a and b present MALLS and RI profiles of the PDMA brush prepared in 3 wt % DMA after 24 and 240 h. The MALLS profile of the sample obtained after 24 h contained a strong shoulder peak at 15 min, which decreased significantly after 240 h of reaction. RI profiles show that the weight ratio of the major peak increased from 96.2% to 99.6% after 240 h

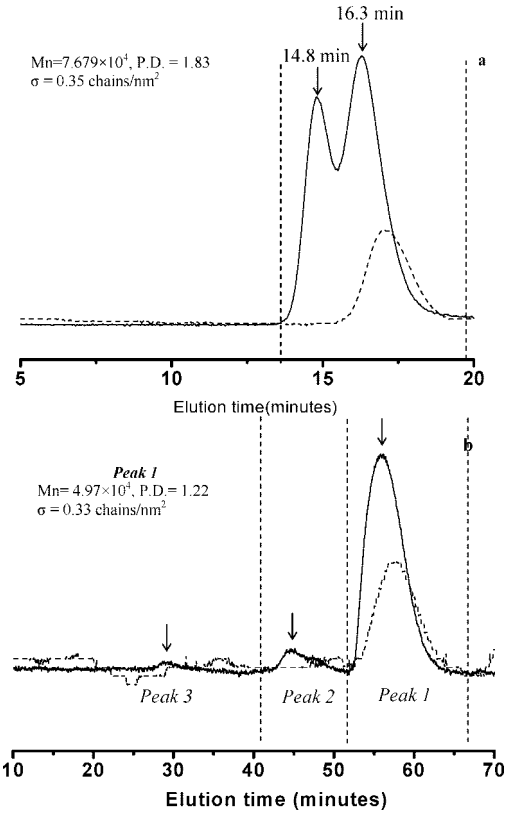

Figure 11. GPC−MALLS (solid line) and refractive index (dashed line) data of cleaved PDMA polymer brushes. GPC of 11a was run through a 2 column setup, while 11b was run through a 4 column setup. ATRP was carried out at room temperature for 72 h. DMA: 2% (w/v). Cu(I) was 2.5 μmol/mL; Cu(II), 3.7 μmol/mL; Cu, 1.5 μmol/mL; HMTETA, 8.7 μmol/mL.

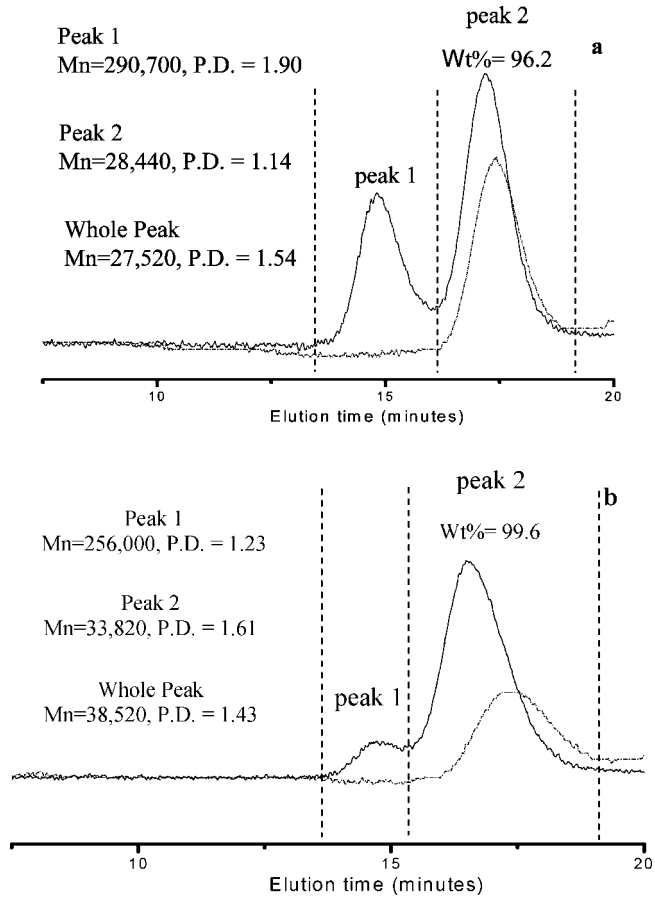

Figure 12. GPC−MALLS (solid line) and RI (dashed line) profiles of PDMA-PVC prepared in 3% DMA after (a) 24 and (b) 240 h. Cu(I) was 2.5 μmol/mL; Cu(II), 3.7 μmol/mL; Cu, 1.5 μmol/mL; HMTETA, 8.7 μmol/mL.

of ATRP. The polydispersity also decreased from 1.54 to 1.43 after 240 h of ATRP. This result indicates that a more uniform surface was obtained with prolonged reaction time. A similar trend was observed in samples prepared in 2 wt % DMA (Figure 6S, Supporting Information).

This time-dependent evolution of the GPC profiles suggests that at the initial stage of polymerization, a small proportion of PDMA chains undergoes uncontrolled polymerization, which gradually becomes minor as more and more chains propagate in a controlled manner with increasing polymerization time. This observation is reminiscent of the initial peak in molecular weight predicted for classical ATRP in the absence of added Cu(II). As the Cu(II) concentration builds up as a result of catalyst cycling the molecular weight comes under control, resulting in a narrowing of the distribution. In our case, excess Cu(II) is always present, however, so this would not be the explanation for the present observation. The reason for it remains obscure and deserves further study.

3.2.6. Control Experiments. To exclude the possibility that solution polymer is being adsorbed onto PVC−CP, control experiments were conducted in which unmodified PVC without ATRP initiator attached were immersed with PVC−CP during ATRP. ATR−FTIR result verified that there was no adsorption of free polymer on the unmodified PVC (data not shown). Another control experiment conducted was aimed at excluding the possibility of free adsorption of ATRP initiators on PVC. Native PVC was reacted with 2-choloropropionyl chloride and polymerized using the same conditions as PVC−ATRP. Again, ATR−FTIR results indicated little PDMA had been grown from the surface. The two control experiments confirmed that PDMA obtained from the PVC surface was absolutely surface-initiated.

Conclusions

The synthesis and methods of characterization described in this paper provide the basis for the systematic study of properties of surface grafted PDMA brushes from a flat PVC sheet. A novel modification strategy was developed to incorporate ATRP initiators and sulfate groups on PVC surface without changing the bulk property of the plastic. For the first time, molecular weight, polydispersity and graft density of a series of PDMA brushes grown on a flat surface were unambiguously characterized by GPC. We found that both monomer concentration and reaction time were important for controlling the molecular weight and graft density. Addition of a Cu(II) complex is critical for obtaining a low polydispersity, while NaCl dramatically reduces graft density. Molecular weights varied from 28 000 to 2 170 000 g/mol and graft density varied from 0.08 to 1.13 chains/nm^2. Values for both molecular weight (2 170 000 Da) and graft density (1.13 chains/nm^2) are the highest reported to date. The high graft densities are likely due to the presence of large amounts of surface initiators; almost four times compared to conventional modification and the presence of sulfate groups on the surface. Surface initiation was found to be a slow process and a long reaction time was required to achieve uniform PDMA brushes. GPC profiles of PDMA brushes prepared in high DMA concentrations show a monomodal peak by MALLS while those prepared in low DMA concentration (≤3%, wt %) have a bimodal peak, indicating nonuniformity of the surface layers caused by uncontrolled polymerization at the initial stage of polymerization.

Acknowledgment. Financial support from CIHR, Canadian Blood Services (CBS) Canada Foundation for Innovation (CFI) and Michael Smith Foundation for Health Research (MSFHR) are gratefully acknowledged. The authors thank Dr. Nicholas Rossi's helpful discussion for the manuscript. The authors thank the LMB Macromolecular Hub at the UBC Center for Blood Research for the use of their research facilities. These facilities are supported in part by grants from the Canada Foundation for Innovation and the Michael Smith Foundation for Health Research. J.N.K. is the recipient of a Canadian Blood Services (CBS)/Canadian Institutes of Health Research (CIHR) new investigator award in transfusion science.

Supporting Information Available: Figures showing ATR−FTIR, UV, XPS, and AFM results for PVC−NH_2, PVC−Sulfate−OH, and PVC−CP and more GPC−MALLS results for PDMA brush. This material is available free of charge via the Internet at http://pubs.acs.org.

References and Notes

(1) Dumitrium, S. *Polymeric Biomaterials*; Marcel Dekker: New York, 1994.
(2) Ratner, B. D.; Castner, D. G. *Surface modification of polymeric materials*; New York, 1997.
(3) Wang, D. A.; Chen, B. L.; Ji, J.; Feng, L. X. *Bioconjugate Chem.* **2002**, *13*, 792–803.
(4) Coelho, M. A.; Vieira, E. P.; Motschmann, H.; Mohwald, H.; Thunemann, A. F. *Langmuir* **2003**, *19*, 7544–7550.
(5) Peter, K.; Schwarz, M.; Contradt, C.; Nordt, T.; Moser, M.; Kubler, W.; Bode, C. *Circulation* **1999**, *100*, 1533–1539.
(6) Videm, V. *Biomaterials* **2004**, *24*, 43–51.
(7) Weber, N.; Wendel, H. P.; Ziemer, G. *Biomaterials* **2002**, *23*, 429–436.
(8) Palkuti, H. S. *J. Med. Tech.* **1985**, *2*, 81–86.
(9) Dumitrium, S. *Polymeric Biomaterials*; Marcel Dekker, Inc.: New York, 2002.
(10) Zhang, C.; Luo, N.; Hirt, D. E. *Langmuir* **2006**, *12*, 6851–6857.
(11) Zdyrko, B.; Klep, V.; Luzinov, I. *Langmuir* **2003**, *19*, 10179–10187.
(12) Wagner, V. E.; Koberstein, J. T.; Bryers, J. D. *Biomaterials* **2004**, *25*, 2247–2263.
(13) Brach, D. W.; Wheeler, B. C.; Brewer, G. J.; Leckband, D. E. *Biomaterials* **2001**, *22*, 1035–1047.
(14) Ye, S. H.; Watanabe, J.; Takai, M.; Iwasaki, Y.; Ishihara, K. *Biomaterials* **2006**, *27*, 1955–1962.
(15) Moro, T.; Takatori, Y.; Ishihara, K.; Konno, T.; Takigawa, Y.; Matsushita, T. *Nat. Mater.* **2004**, *3*, 829–836.
(16) Ye, S. H.; Watanabe, J.; Iwasaki, Y.; Ishihara, K. *Biomaterials* **2003**, *24*, 4143–4152.
(17) Iwata, R.; Suk-In, P.; Hoven, V. P.; Takahara, A.; Akiyoshi, K.; Iwasaki, Y. *Biomacromolecules* **2004**, *5*, 2308–2314.
(18) Unsworth, L. D.; Sheardown, H.; Brash, J. L. *Langmuir* **2005**, *21*, 1036–1041.
(19) Feng, W.; Brash, J. L.; Zhu, S. *Biomaterials* **2006**, *27*, 847–855.
(20) Janzen, J.; Le, Y.; Kizhakkedathu, J. N.; Brooks, D. E. *J. Biomater. Sci.* **2004**, *15*, 1121–1135.
(21) Dronnavajjala, K. D.; Rajagopalan, R.; Uppili, S.; Sen, A.; Allara, D. L.; Foley, H. C. *J. Am. Chem. Soc.* **2006**, *128*, 13040–13041.
(22) Matyjaszewski, K.; Miller, P. J.; Shukla, N.; Immaraporn, B.; Gelman, A.; Luokala, B. B.; Sichlovan, T. M.; Kickelbick, G.; Vallant, T.; Hoffmann, H.; Pakula, T. *Macromolecules* **1999**, *32*, 8716–8724.
(23) Jordan, R.; Ulman, A.; Kang, J. F.; Rafaiovich, M. H.; Sokolov, J. *J. Am. Chem. Soc.* **1999**, *121*, 1016–1022.
(24) Jordan, R.; Ulman, A. *J. Am. Chem. Soc.* **1998**, *120*, 243–247.
(25) Week, M.; Jackiw, J. J.; Rossi, R. R.; Weiss, P. S.; Grubbs, R. H. *J. Am. Chem. Soc.* **1999**, *121*, 4088–9.
(26) Hyun, J.; Chilkoti, A. *Macromolecules* **2001**, *34*, 5644–5652.
(27) Bian, K.; Cunningham, M. F. *Polymer* **2006**, *47*, 5744–5753.
(28) Perrier, S.; Takolpuckdee, P.; Mars, C. A. *Macromolecules* **2005**, *38*, 6770–6774.
(29) For a review of ATRP, please refer to the following: (a) Matyjaszewski, K.; Xia, J. *Chem. Rev.* **2001**, *101*, 2921 90;(b) Kamigaito, M.; Ando, T.; Sawamoto, M. *Chem. Rev.* **2001**, *101*, 3689–3754. For a review of polymer brushes, please refer to the following: (c) Edmondson, S.; Osborne, V. L.; Huck, W. T. S. *Chem. Soc. Rev.* **2004**, *33*, 14–23. (d) Tsujii, Y.; Ohno, K.; Yamamoto, S.; Goto, A.; Fukuda, T. *Adv. Polym. Sci.* **2006**, *197*, 1–45.
(30) Singh, N.; Cui, X.; Boland, T.; Husson, S. M. *Biomaterials* **2007**, *28*, 763–771.
(31) Gao, C.; Muthukrishnanan, S.; Li, W.; Yuan, J.; Xu, Y.; Muller, A. H. E. *Macromolecules* **2007**, *40*, 1803–1815.
(32) Muthukrishnan, S.; Erhard, D. P.; Mori, H.; Muller, A. H. E. *Macromolecules* **2006**, *39*, 2743–2750.
(33) Plunkett, K. N.; Zhu, X.; Moore, J. S.; Leckband, D. E. *Langmuir* **2004**, *22*, 4259–4266.
(34) Kong, H.; Li, W.; Gao, C.; Yan, D.; Jin, Y.; Walton, D. R. M.; Kroto, H. W. *Macromolecules* **2004**, *37*, 6683–6686.
(35) Kizhakkedathu, J. N.; Jones, R. N.; Brooks, D. E. *Macromolecules* **2004**, *37*, 734–743.
(36) Feng, W.; Brash, J. L.; Zhu, S. *Biomaterials* **2006**, *27*, 847–855.
(37) Wang, Y.; Hu, S.; Brittain, W. J. *Macromolecules* **2006**, *39*, 5675–5678.
(38) Xu, C.; Wu, T.; Mei, Y.; Drain, C. M.; Batteas, J. D.; Beers, K. L. *Langmuir* **2005**, *21*, 11136–11140.
(39) Huang, W.; Kim, J. B.; Bruening, M. L.; Baker, G. L. *Macromolecules* **2002**, *35*, 1175–1179.
(40) Huang, X.; Wirth, M. J. *Macromolecules* **1999**, *32*, 1694–1696.
(41) Jayachandran, K. N.; Cox, A. T.; Brooks, D. E. *Macromolecules* **2002**, *35*, 4247–4257.
(42) Kizhakkedathu, J. N.; Brooks, D. E. *Macromolecules* **2003**, *36*, 591–598.
(43) Santer, S.; Kopyshev, A.; Yang, Y. K.; Ruhe, J. *Macromolecules* **2006**, *39*, 3056–3064.
(44) Ejaz, M.; Yamamoto, S.; Ohno, K.; Tsujii, Y.; Fukuda, T. *Macromolecules* **1998**, *31*, 5934–5936.
(45) Husseman, M.; Malmstrom, E. E.; Mcnamara, M.; Mate, M.; Mecerreyes, D.; Benoit, D. G.; Hedrick, J. L.; Mansky, P.; Huang, E.; Russell, T. P.; Hawker, C. J. *Macromolecules* **1999**, *32*, 1424–1431.
(46) Ejaz, M.; Ohono, K.; Tsujii, Y.; Fukuda, T. *Macromolecules* **2000**, *33*, 2870–2874.
(47) Yamamoto, S.; Ejaz, M.; Tsujii, Y.; Fukuda, T. *Macromolecules* **2000**, *33*, 5608–5612.
(48) Lamba, N. M. K.; Courtney, J. M.; Gaylor, J. D. S.; Lowe, G. D. O. *Biomaterials* **2000**, *21*, 89–96.
(49) Hong, J.; Ekdahl, K. N.; Reynolds, H.; Larsson, R.; Nilsson, B. *Biomaterials* **1999**, *20*, 603–611.
(50) Balakrishnan, B.; Kumar, D. S.; Yoshida, Y.; Jayakrishnan, A. *Biomaterials* **2005**, *26*, 3495–3502.
(51) Labarta, J. R.; Herrero, M.; Tiemblo, P.; Mijangos, C.; Reinecke, H. *Polymer* **2003**, *44*, 2263–2269.
(52) Pruker, O.; Ruhe, J. *Macromolecules* **1998**, *31*, 592–601.
(53) Teodorescu, M.; Matyjaszewski, K. *Macromolecules* **1999**, *32*, 4826–4831.
(54) Butt, H. J.; Kappl, M.; Mueller, H.; Raiteri, R. *Langmuir* **1999**, *15*, 2559–2565.
(55) Cuenot, S.; Gabriel, S.; Jerome, R.; Jerome, C.; Fustin, C. A.; Jonas, A. M.; Duwez, A. S. *Macromolecules* **2006**, *39*, 8428–8433.
(56) Devaux, C.; Chapel, J. P.; Beyou, E.; Chaumont, P. *Eur. Phys. J. E* **2002**, *7*, 345–352.
(57) Maeng, S.; Park, J. W. *Langmuir* **2003**, *19*, 4519–4522.
(58) Ejaz, M.; Yamamoto, S.; Tsujii, Y.; Fukuda, T. *Macromolecules* **2002**, *35*, 1412–1418.
(59) Ducker, W. A.; Sendan, T. J.; Pashley, R. M. *Langmuir* **1992**, *8*, 1831–1836.
(60) Goodman, D.; Kizhakkedathu, J. N.; Brooks, D. E. *Langmuir* **2004**, *20*, 3297–3303.
(61) Sumerlin, B. S.; Neugebauer, D.; Matyjaszewski, K. *Macromolecules* **2005**, *38*, 702–708.
(62) Tsarevsky, N. V.; Pintauer, T.; Glogowski, E.; Matyjaszewski, K. *Polym. Prep.* **2002**, *43*, 201–202.
(63) Jewrajka, S. K.; Mandal, B. M. *Macromolecules* **2003**, *36*, 311–317.

MA8025699